

Clinical Significance and Classification Pattern of Ventricular Bands in The Heart of Domestic Cats (*Felis catus*): An Echocardiographic and Morphometric Study

Maher M.A.^a and Samar H. Elsharkawy^b

^a Department of Anatomy and Embryology, Faculty of Veterinary Medicine, Cairo University, Giza Square, P.O. 12211, Cairo, Egypt.

^b Department of Surgery, Anesthesiology and Radiology, Faculty of Veterinary Medicine, Cairo University, Giza Square, P.O. 12211, Cairo, Egypt.

With 3 tables & 11 figures. Received October, accepted for publication November

Abstract

The present investigation was carried out on cardiac ventricles of fourteen adult Egyptian domestic cats of both sexes after physical and ultra-sonographic examination to identify, schematically classify and echocardiographically assess the ventricular musculo-fibrous or moderator bands a or septomarginal trabeculae. The bands are classified according to insertion points into six types I, II, III, IV, V, and VI, and subtypes of Ia, Ib, Ic, IIa, IIb, Va, Vb, VIa, and VIb. The M. papillaris magnus was the largest and the Mm. papillares parvi were found two or three in the right ventricle where they were inserted in the septum. The two papillary muscles of the left ventricle were at the same size except in one cat where the papillary subatrialis was twice larger than the sub-auricularis. The trabeculae carneae form deep spaces in the right ventricles and shallow ones in the left ones. Echocardiographically, ventricular bands of the right ventricle were

difficult to appear while in the left ventricle, there was one cat showed the presence of an echogenic fibromuscular band connecting the left ventricular apex and the ventricular septum.

In conclusion: Bands of subtypes Ib, Ic, and Vb were absent in the right ventricles While, Ia, Ib, and Va were absent in left ventricles. The echocardiographic evidence of the ventricular bands revealed no interference to the ventricular contractility based on the assessment of the systolic and diastolic function.

Keywords: Cat, Echocardiography, Heart, Morphometry, Septomarginal trabeculae, Moderator bands

Introduction

The heart possesses a signaling system that causes regular contractions on its own, without the aid of external triggers, and the contraction velocity is motivated by the autonomic nervous system through pulsation. This system is constituted of sinuatrial

node, atrio-ventricular node, His bundles, and Purkinje fibers. The sinoatrial node impulse propagates to the atrio-ventricular node, then to His bundles, and lastly to Purkinje fibers in the right and left ventricular walls, where it is dispersed in the myocardium (Noyan, 1998; Özer, 2008; Padala, et al., 2021; Erdem et al., 2022).

Septomarginal trabeculae (moderator bands) are known as a thin, band-like structure, connecting the inter-ventricular septum or papillary muscles to the ventricular free wall. They are always found in the right ventricle but rarer in the left one, preventing a great strain during ventricular diastole (Fox, 1999; Wray et al., 2007; Parto et al., 2010; Dyce et al., 2010; Evans & de Lahunta, 2013). These trabeculae and their Purkinje fibers are of the same structures in both human and animal right ventricles, although there are individual variances in the left ventricle (Ghonimi et al., 2014; Ates et al., 2017).

Typical chordae tendineae are fibromuscular cords that proceed from the atrioventricular valve cusps to the papillary muscle apices (Evans, 1993). In canine hearts, two studies described false chordae tendineae as anomalous in the right ventricle. In the first, the chordae tendineae extends from a valve cusp to the ventricular free wall (Costa et al., 1999). While in the second, the chordae tendineae are attached to the ring of the atrioventricular valve or the intermediate

semilunar valve of the pulmonary trunk and inserted into an associated papillary muscle (Costa et al., 2000).

The excessive moderator bands in the left ventricle are considered a rare congenital anomaly in domestic cats (Fox, 1999; Wray et al., 2007) also when presented in excess in the left ventricle, they are associated with heart diseases such as arrhythmias (Sadek et al., 2015; Lerman et al., 2018; Barber et al., 2019) or innocent heart murmurs (Koie et al., 2007). The abnormal diffuse networks of excessive moderator bands have been reportedly associated with heart failure and death (Liu & Fox, 1999).

Hypertrophic cardiomyopathy is the most common heart disease in cats and is characterized by ventricular hypertrophy and both diastolic and systolic dysfunction which leads to enlargement and subsequent congestive heart failure (Ferasin et al., 2003; Paige et al., 2009; Wilkie et al., 2015). So, the development of echocardiography appears to have reawakened interest in a variety of cardiac conditions (Abdulla et al., 1990; Kervancioglu et al., 2003).

The aim of our study is first, to morphologically illustrate the structures of the right and left ventricles that control the ventricular filling, especially the chordae tendineae, the septomarginal trabeculae or moderator bands, and construct a classification scheme according to their shape and pattern

of distribution. Secondly, to echocardiographically assess the normal ven-tricular wall thickness, interven-tricular septum thickness, chamber di-mension, fractional shortening, ejec-tion fraction, mitral inflow E wave ve-locity, mitral inflow A wave velocity, mitral inflow E wave to A wave ratio, peak aortic velocity and function in healthy cats.

Material and Methods

The Anatomical Studies

The morphoanatomical investigation of the present study was carried out on the cardiac ventricles of eight adult Egyptian domestic cats of both sexes that appeared healthy by physical and ultrasonographic examination. Hearts were obtained from the examined cats after sedation with xylazine (1mg/kg), and ketamine (20mg/kg) and overcoming the pain using an overdose of sodium thiopental 2.5% then exsanguination following the rules established by the institutional animal care and use committee. The clearing of remaining cardiac and vascular blood was performed by fixing a cannula through the common carotid artery and draining through the jugular vein using phosphate-buffered saline of 0.9% followed by a buffered formalin solution of 10%. Hearts were removed from the thorax then rinsed in a physiological solution. After that, hearts were studied outside the thorax and pericardium. Specimens

were then subjected to examination through anatomical dissection where the right ventricle was incised by two lines parallel to the coronary and lon-gitudinal grooves. While, the left ven-tricle was incised by a single mid-line incision from the coronary groove till reaching the apex. Our present work has been approved by the institutional animal care and use committee (IACUC) of Cairo University allocated the IACUC number (VET CU 03162023657). Moreover, we con-firmed that all methods were per-formed in accor-dance with the rele-vant guidelines and regulations. All macroscopic anatomical illustrations were recorded and photographed using a digital photo camera Nikon Cool-pix L310 14.1 Megapixels. The nomen-clature used in this study was adopted according to Nomina Ana-tomica Veterinaria (2017).

The Echocardiographic Studies

Apparently healthy six cats that showed normal clinical and echo-car-diographic examination were included in the study. Cats were randomly cho-sen among the population admitted to the surgery department at the Small Animal Teaching Hospital, Faculty of Veterinary Medicine, Cairo Uni-ver-sity. Doppler echocardiography had been carried out by a single examiner (SE) with a Hitachi Aloka F31 ultra-sound machine equipped with a phased array transducer; a frequency range of 5.5 to 8 MHz. All standard echocardiographic views were

obtained, and measurements were applied following previous protocols (Thomas et al., 1993). Echocardiographic assessment of the patient as "normal" was made as previously conducted (Koffas et al., 2006; Riesen et al., 2007; Linney et al., 2014) and any cat showing structural or functional abnormality was excluded. All cats were examined for the presence of fibrous /fibro-muscular or moderator bands traversing the left ventricular cavity with no connection to the mitral valve leaflets.

The Statistical and Morphometric Analysis

The mean value \pm standard error (SE) and standard deviation (SD) with variance were analyzed using IBM SPSS statistics software (2007) and tabulated with accurate reference ranges for each parameter. A significant difference was detected when $p < 0.05$.

Results

The Anatomical and Morphometric Studies:

The external contour of cat's heart appeared rounded in outline (Fig. 1). Its vertical distance between the aortic arch and apex, the cranio-caudal dimension at the heart base, the conus arteriosus diameter, the distances from most ventral left and right auricular borders to apex, the diameter of both right atrioventricular orifice and ventricle and the average length of *Musculus papillaris magnus's*

chordae tendineae were measured using a Vernier caliper and statistically analyzed then tabulated in (table 1 and 2).

The anatomical conformational structure of cat's right ventricle was constituted of the right atrio-ventricular orifice that bounded at its inner aspect by three valve cusps (*Valva tricuspidalis*); *Cusps septalis*, *Cusps parietalis*, and *Cusps angularis*. These cusps were attached, by thin tendon-like filaments called chordae tendineae (Fig. 2/CT), to three muscular protrusions elevated from the interventricular septum which called *Mm. papillares*; *Musculus papillaris magnus*, *Musculi papillares parvi* and *Musculus papillaris subarteriosus* (Fig. 2). Dorsally, the beginning of the pulmonary trunk (*Conus arteriosus*) was bounded medially by *Crista supraventricularis*. Ventrolaterally, numerous deep trabecular spaces called *trabeculae carneae* (Fig. 2/TC) were situated in the septal and ventricular free walls.

The left ventricular structures (Fig. 6-9) resemble that of the right ventricle with some modifications. The left atrio-ventricular orifice contains two valve cusps (*Valva bicuspidalis*, *mitralis*); *Cusps septalis* and *Cusps parietalis*. The aortic orifice instead of the pulmonary orifice. The chordae tendineae are attached to only two thick *Mm. papillares*; *Musculus papillaris subauricularis* and *M. papillaris subatrialis* (Fig. 6).

The septomarginal trabeculae or moderator bands (Fig. 3); are thin, band-like structures, connecting the interventricular septum or papillary muscles to the ventricular free wall without any connection with the atrioventricular valve cusps. They are responsible for carrying the conducting pulsation tissue; Purkinje fibers, for coordinated contraction of all parts of the ventricles. These ventricular bands are more excessive in the right ventricle than the left one, with different locations, numbers, diameters, lengths, and patterns of distribution. So, the present study established a schematic classification to these ventricular bands in both ventricles as follows; I: bands from interventricular septum to ventricular free wall (Fig.2/A), II: from the papillary muscles to ventricular free wall (Fig.3), III: connecting between the septal trabeculae carneae (Fig.4/B), IV: connecting between free wall trabeculae carneae (Fig.3-5/B), V: interconnecting between the papillares parvi (Fig. 4/B) and papillaris magnus or between subauricularis and subatrialis (Fig. 8), VI: connecting ventricular septum to papillary muscles (Fig. 4-7)).

A subdivision to the previous classification scheme was observed in the cats heart according to number of insertion points as follows; Ia: Y-shaped trabeculae with two points of insertion (Fig. 3A), Ib: web-like trabeculae with 3-4 points of insertion, Ic: web-like

trabeculae with 5 or more points of insertion (Fig. 7-8-9), IIa: Y-shaped trabeculae with two points of insertion (Fig. 3A-4), IIb: web-like trabeculae with 3-4 points of insertion (Fig. 2B-6), Va: connecting two papillares parvi (Fig. 4B), Vb: connecting different papillary muscles (Fig. 8), VIa: trabeculae between ventricular septum and papillares parvi (Fig. 4A) or subauricularis muscles (Fig. 6), VIb: trabeculae between ventricular septum and papillaris magnus (Fig. 2A) or subatrialis muscles (Fig. 7).

In the right ventricle (*Ventriculus dexter*); the *M. papillaris magnus*, is considered the largest papillary muscle located in the middle of the right ventricle parallel to the long axis of the heart, its apical extremity received 2-7 filamentous bundles of chordae tendineae. While its basal extremity either inserted in the distal free wall (Fig. 2A) in 3 hearts (37.5%) or inserted in distal interventricular septum (Fig. 5) in 5 hearts (62.5%). The papillary parvi muscles were smaller than the magnus located in the left caudolateral portion and oblique in direction, their numbers were 2 muscles in 6 hearts (75%) and 3 muscles (Fig. 2A) in two hearts (25%), received 3-4 filamentous bundles of chordae tendineae and all inserted in the ventricular septum. The papillary subarteriosus muscle (Fig. 3B/ps) was very small and conical in shape located on the upper ventricular septum, and ventral to the pulmonary opening,

received 2-3 bundles of chordae tendineae.

In the left ventricle (*Ventriculus sinister*); in all examined cats heart, the papillary subauricularis muscle (Fig. 6/p.sau) was located ventral to the left auricle attached to *Cuspis parietalis*. While the papillary sub-atrialis (Fig. 6/p.sat) muscle was ventral to the left atrium attached to *Cuspis septalis*. These two papillary muscles were situated on the parietal wall and not related to the inter-ventricular septum (Fig. 6-7-8-9). Their size is distinct, large thick, and covered a relatively great area of the ventricular wall except in one heart, where the papillary subatrialis was twice larger than the papillary subauricularis (12.5%) (Fig. 9/p.sat). They received 7-10 filamentous bundles of chordae tendineae on the apical portions of each.

Other than cord-like filaments of atrio-ventricular valve cusps (chordae tendineae), there are thick ribbon-like musculo-tendinous bands were found in the right ventricle only in two examined hearts, connecting the outer aspect of parietal valve cusps to the ventricular free wall that considered as false chordae tendineae (Fig. 5/FCT) and overlapping the papillares parvi muscles.

Types of ventricular bands or septo-marginal trabeculae that were found in the cat right ventricle were type I, Ia, II, IIa, IIb, III, IV, Va, VIa and VIb with conspicuous trabeculae carneae

in both septal and free ven-tricular walls. While, the ventricular bands observed in the left ventricles were type I, Ic, II, IIa, IIb, III, IV, Vb, VIa, and VIb with shallow or not clear trabeculae in both septal and ventricular free walls with a characteristic branching pattern of subtype Ic (Fig. 9/Strikes). Whenever most of the left ventricular bands were found thick and forming web or net-like trabeculation which often communicate with each other (Fig. 7/Strike).

The Echocardiographic Studies:

A total of six cats were included in our present study. The demographic and echocardiographic data of the study population are summarized in (Table 3). Among the six examined cats, the ventricular bands of the right ventricle were difficult to appear. While in the left ventricle, there was one cat showed the presence of an echogenic fibromuscular band connecting the left ventricular apex and the ventricular septum (Fig. 10-11).

Discussion

The Anatomical and Morphometric Studies:

Our present investigation of the cat's right ventricular structures revealed a size variability of the three identified papillary muscles, where the papillary magnus was the largest muscle followed by the papillary parvi. Then the smallest conical-shaped papillary subarteriosus muscle. However,

previous literature stated that the papillary magnus and subarteriosus had similar sizes (Perez & Lima, 2007) in tigers, the papillary magnus was the well-developed (Evans, 1993; Barone, 1996) in dogs while the papillary subarteriosus was the most prominent muscle (Barone, 1996) in cats.

Concerning the left ventricular papillary muscles, Perez and Lima (2007) in tigers and Evans (1993) in dogs reported that the papillary subauricularis was the largest papillary muscle of the left ventricle. Although, Barone (1996) in cats confirmed that the papillary subatrialis was the greatest muscle. While, our present study revealed the same size of both muscles in the majority of specimens except in one cat out of eight with a percentage of (12.5%) where the papillary subatrialis was twice larger than the papillary sub-auricularis muscle.

Trabeculae carneae in the current investigation were characteristic, constituting a great trabeculation with deep spaces either in the septal or outer free walls of the right ventricle but these trabeculae were not clear with shallow depressions in the left ventricle. However, they were extensive and well-developed occupying a great area in both the septal and parietal walls of the right and left ventricles (Perez & Lima, 2007; Kosiński et al., 2010).

In Eurasian lynx (Kareinen et al., 2020), gazelle (Erdem et al., 2022),

and humans (Kosiński et al., 2010), the papillary magnus muscle was located either centrally or parietally and inserted in the distal ventricular free wall while the papillary sub-auricularis inserted in the parietal wall and subatrialis inserted in the septal wall. But the present study revealed a centrally located papillary magnus muscle that was either inserted in the septum (62.5%) or in the distal free wall (37.5%) while the papillary subauricularis and sub-atrialis were distinct and strictly inserted in the left ventricular free wall and occupied a great area in all studied cats.

In previous literature, the septo-marginal trabeculae or moderator bands revealed variability in the distribution pattern. Kosiński et al. (2010, 2013) in humans and primates stated four types of ventricular bands; type I, II, and III running from the ventricular septum to the ventricular free wall without division. While type IV septo-marginal trabecula was divided by the papillary magnus muscle into two parts, septopapillary and papillo-marginal. The latter was subdivided into three subtypes; IVa, IVb, and IVc. The latter subtype IVc was diverse and branched toward the ventricular free wall. A completely different pattern was established by Cope (2016b) in dogs according to the trabecular attachment and insertion points into four types; I, which was a band with a single point of insertion, Ia, Y-shaped with two insertion points, Ib, web-like

with 3-4 insertion points, and Ic, web-like with 5 or more insertion points.

The present study revealed a classification scheme concerning the septomarginal trabeculae in the right and left ventricles of the cat which is characterized as I, Ia, Ib, Ic, II, IIa, IIb, III, IV, V, Va, Vb, VI, VIa and VIb that was similar to the observations of **Cope (2017)** in the right ventricle of dogs. However, our current investigation in the cat revealed the occurrence of types; I, Ia, II, IIa, IIb, III, IV, Va, VIa, and VIb in the right ventricle and types; I, Ic, II, IIa, IIb, III, IV, Vb, VIa and VIb in the left ventricle.

Concerning the papillomarginal distribution pattern of the septomarginal trabeculae in both ventricles, the most predominant types in the cats of the present study were type II followed by IIa and IIb for the right ventricle and type II followed by IIa in the left ventricle. While, Cope (2016b) reported that the most predominant types in the right ventricle were type Ic followed by Ib then I and Ia in all studied dogs.

Kareinen et al. (2020) in Eurasian lynx reported that the papillomarginal ventricular bands were more numerous in the left ventricle than in the right one. Furthermore, Erdem et al. (2022) confirmed the reports of Kareinen et al. and added that these ventricular bands were found in the right ventricle with a percentage of (18%) and in the left one with a percentage of (71%) of

examined gazelle hearts. While in the present investigation of cats, the right papillomarginal bands were observed more numerous and common finding in the right ventricle with a percentage of (87.5%) and in the left ventricle with a percentage of (37.5%) of examined cats heart. Our observations were in accordance with Lee and Hur (2019) in humans, Ates et al. (2017) in pigs, Ghonimi et al. (2014) in buffalos, Cope (2016b) in dogs, Kareinen et al. (2020) in lynx and Erdem et al. (2022) in gazelle who reported that the number of septomarginal band of type I in the right ventricle was one. In some literature, these bands were two by Vazquez et al. (2019) in Pampas's deers, and three by Ateş and Çakır (2010) in rabbits.

Chordae tendineae in dogs were reported as cords connecting the ventral margin of the atrioventricular valve cusp to the apices of the papillary muscles (Evans, 1993). The present study revealed a musculo-fibrous ribbon-like band, in the right ventricle only, connecting the ring of the atrioventricular valve to the ventricular free wall, representing (25%) of examined cat hearts and did not be observed in the left ventricle which was described as false (atypical) chordae tendineae. The results were supported by (Costa et al., 1999) in mongrel dog; (Loukas et al., 2008) in human; (Cope, 2016a) in dogs. Whenever, Moreno et al. (2003) in human linked these atypical tendineae

with the presence of cardiac pathologies and catheter-ization entanglement in human hearts.

The ventricular bands of the current study, specific to the septal trabeculae carnae (III) representing 62.5% and 25% in the right and left ventricles respectively, and those related to the free wall trabeculae carnae (IV) representing 37.5% and 12.5% in the right and left ventricles respectively. While in dogs, type III represents 12.9%, and type IV represents 11.7% of all examined hearts (Cope, 2017). In addition to the subtype VIa, connecting the ventricular septum either to the papillary parvi or subauricularis muscles, and subtype VIb, connecting the ventricular septum either to the M. papillaris magnus or M. subatrialis (Cope, 2017) in dogs.

The Echocardiographic Studies:

Among the study population, a single cat showed echocardiographic evidence of the ventricular bands with a close resemblance to the previous reports in healthy cats (Wolf et al., 2017). This band showed no interference to the left ventricular contractility based on the assessment of the systolic and diastolic function.

Conclusion

Being a small animal, the cat is recently used in ventricular septal defect repair, heart transplantation, monitoring and diagnosing pulmonary hypertension, and stem cell

research by delivering the stem cells to the endocardium of the heart using specialized cell inoculating catheters. It is very interesting for clinicians to have a well-knowledge of the feline ventricular structural morphology especially, the traversing trabeculae and bands which are found highly variable and taking different patterns of distribution varying from single strand, y-shaped to web or net-like insertion points that must be reported to bypass the prospective trabecular damage and catheter entanglement during lead pacemaker positioning which is the most common complication or to evolve techniques for unentanglement.

Ethics Approval

This work has been approved by the Institutional animal care and use committee (IACUC) with IACUC number (VET CU 03162023657).

Conflict of Interest

The authors have no conflict of interest.

Data Availability Statement

The data that support the findings of this study are available from the corresponding author upon reasonable request.

ORCID

Maher MA

<https://orcid.org/0000-0002-7040-7813>

Elsharkawy SH

<https://orcid.org/0000-0002-9496-6601>

References

Abdulla, A. K., Frustaci, A., Martinez, J. E., Florio, R. A., Somerville, J. & Olsen, E. G. J. (1990): Echocardiography and pathology of left ventricular false tendons. *Chest*, 96, 129–132.

<https://doi.org/10.1378/chest.98.1.129>

Ateş, S. & Çakır, A. (2010): Yeni Zelanda tavşanı ve kobaydaki kalp kapaklarının karşılaştırmalı makroanatomisi. *Ankara Üniversitesi Veteriner Fakültesi Dergisi*, 57, 145–150.

https://doi.org/10.1501/Vet-fak_0000002367

Ateş, S., Karakurum, E., Takcı, L., Başak, F. & Kürtül, İ. (2017): Morphology of the atrioventricular valves and related intraventricular structures in the wild pig (*Sus scrofa*). *Folia Morphologica*, 76, 650–659.

<https://doi.org/10.5603/FM.a2017.0051>

Barber, M., Chinitz, J. & John, R. (2019): Arrhythmias from the right ventricular moderator band: Diagnosis and management. *Arrhythmia & Electrophysiology Review*, 8, 294–299.

<https://doi.org/10.15420/aer.2019.18>

Barone, R. (1996): Anatomie comparée des mammifères domestiques. Tome 5. Angiologie. éditions Vigot, Paris. 91–95.

Cope, L. A. (2016a): Atypical chordae tendineae of the canine (*Canis familiaris*) right atrioventricular valve. *Anatomia, Histologia, Embryologia*, 45, 485–489.

<https://doi.org/10.1111/ahe.12231>

Cope, L. A. (2016b): Morphological variations in the canine (*Canis familiaris*) right ventricle trabecula septomarginalis dextra and a proposed classification scheme. *Anatomia, Histologia, Embryologia*, 45, 437–442.

<https://doi.org/10.1111/ahe.12217>

Cope, L. A. (2017): Morphology and classification of right ventricular bands in the domestic dog (*Canis familiaris*). *Anatomia Histologia and Embryologia*, 46, 464–473.

<https://doi.org/10.1111/ahe.12291>

Costa, F. S., Appolinario, A. V. M., de Morais-Pinto, L. & de Oliveira, A. (1999): A special type of chordae tendineae in the right ventricle of the mongrel dog (*Canis familiaris*). *Braz. J. Morphol. Sci.*, 16, 217–18.

Costa, F. S., de Morais-Pinto, L., Appolinario, A. V. M. & de Oliveira, A. (2000): The anomalous tendinous cord in the right atrioventricular valve in mongrel dogs (*Canis familiaris*). *Braz. J. Vet. Res. Anim. Sci.*, 37, 1–3.

Dyce, K. M., Sack, W. O. & Wensing, C. J. G. (2010): Text-book of veterinary anatomy. St. Louis, MO: Elsevier.

Erdem, B., Tutar, T., Takcı, L., Akaydin Bozkurt, Y. & Ateş, S. (2022): Morphology of septomarginal trabeculae in Hatay mountain gazelle (*Gazella gazella*). *Anatomia, Histologia, Embryologia*, 51, 189–196.

<https://doi.org/10.1111/ahe.12777>

Evans, H. E. (1993): Miller's Anatomy of the Dog. Philadelphia: W. B. Saunders Company.

Evans, H. E. & de Lahunta, A. (2013): Miller's anatomy of the dog. St. Louis, MO: Elsevier.

Ferasin, L., Sturgess, C. P., Cannon, M. J., Caney, S. M., Gruffydd-Jones, T. J. & Wotton, P. R. (2003): Feline Idiopathic Cardiomyopathy: A Retrospective Study of 106 Cats (1994-2001). *Journal Feline Medicine Surgery*, 5, 151-159.

[https://doi.org/10.1016/S1098-612X\(02\)00133-X](https://doi.org/10.1016/S1098-612X(02)00133-X)

Fox, P. R. (1999): Feline cardiomyopathies. In: *Textbook of Canine and Feline Cardiology*, 2nd ed. (P. R. Fox, D. Sisson and N. E. Moise, eds). Philadelphia: W.B. Saunders. pp. 621-678.

Ghonimi, W., Abuel-Atta, A. A., Bareedy, M. H. & Balah, A. (2014): Gross and microanatomical studies on the moderator bands (septo-marginal trabecula) in the heart of mature Dromedary camel (*Camelus dromedarius*). *Journal of Advanced Veterinary and Animal Research*, 1, 24-31. <https://doi.org/10.5455/javar.v1i2p24-31>

Kareinen, I., Lavonen, E., Viranta-Kovanen, S., Holmala, K. & Laakkonen, J. (2020): Anatomical variations and pathological changes in the hearts of free-ranging Eurasian lynx (*Lynx lynx*) in Finland. *European Journal of Wildlife Research*, 66, 21. <https://doi.org/10.1007/s10344-019-1350-y>

Kervancioglu, M., Ozbag, D., Kervancioglu, P., Hatipoglu, E. S., Kilinc, M., Yilmaz, F. & Deniz, M. (2003): Echocardiographic and morphologic examination of left ventricular false tendons in humans and animal hearts. *Clinical Anatomy*, 16, 389-395.

Koffas, H., Dukes-McEwan, J., Corcoran, B. M., Moran, C. M., French, A., Sboros, V. & McDicken, W. N. (2006): Pulsed tissue Doppler imaging in normal cats and cats with hypertrophic cardiomyopathy. *Journal of Veterinary Internal Medicine*, 20, 65-77.

Koie, H., Hara, A., Sakai, M., Takiyama, N. & Uechi, M. (2007): Clinical Evaluation of Left Ventricular Moderator Band in 12 Dogs. *Journal Veterinary Medicine Science*, 69, 965-967.

<https://doi.org/10.1292/jvms.69.965>

Kosiński, A., Kozłowski, D., Nowinski, J., Lewicka, E., Dabrowska-Kugacka, A., Raczak, G. & Grzybiak, M. (2010): Morphogenetic aspects of the septomarginal trabecula in the human heart. *Archives of Medical Science*, 6, 733-743. <https://doi.org/10.5114/aoms.2010.17089>

Kosiński, A., Zajaczkowski, M., Kuta, W., Kozłowski, D., Szpinda, M. & Grzybiak, M. (2013): Septomarginal trabecula and anterior papillary muscle in primate hearts: Developmental issues. *Folia Morphologica*, 72, 202-209.

<https://doi.org/10.5603/fm.2013.0034>

Lee, J. Y. & Hur, M. S. (2019): Morphological classification of the moderator band and its relationship with the

anterior papillary muscle. *Anatomy & Cell Biology*, 52, 38–42.
<https://doi.org/10.5115/acb.2019.52.1.38>

Lerman, B. B., Cheung, J. W., Ip, J. E., Liu, C. F., Thomas, G. & Markowitz, S. M. (2018): Mechanistic subtypes of focal right ventricular tachycardia. *Journal of Cardio-vascular Electrophysiology*, 29, 1181–1188.
<https://doi.org/10.1111/jce.13505>

Linney, C. J., Dukes-McEwan, J., Stephenson, H. M., López-Alvarez, J. & Fonfara, S. (2014): Left atrial size, atrial function and left ventricular diastolic function in cats with hypertrophic cardiomyopathy. *Journal of Small Animal Practice*, 55, 198–206.

Liu, S. K. & Fox, P. R. (1999): Cardiovascular pathology. In: *Text-book of Canine and Feline Cardiology*, 2nd edn. (P. R. Fox, D. Sisson and N. E. Moise, eds). Philadelphia: W. B. Saunders. pp. 817–844.

Loukas, M., Wartmann, C. T., Shane Tubbs, R., Apaydin, N., Jr Louis, R. G., Black, B. & Jordan, R. (2008): Right ventricular false tendons, a cadaveric approach. *Surg. Radiol. Anat.*, 30, 317–322.

Moreno, R., Zamorano, J., Ortega, A., Villate, A., Almeria, C., Herrera, D., Rodrigo, J. L., Morales, R. & Sanchez-Harguindey, L. (2003): Tricuspid valve chordae rupture following pacemaker electrode replacement. *Int. J. Cardiol.*, 87, 291–292.

Noyan, A. (1998): Yaşam Davehekimlikte fizyoloji (7. Baskı) Ankara, Meteksan.

Özer, A. (2008): Veteriner özel-histoloji. Dora Yayıncılık.

Padala, S. K., Cabrera, J. A. & Ellenbogen, K. A. (2021): Anatomy of the cardiac conduction system. *Pacing and Clinical Electro-physiology*, 44, 15–25.
<https://doi.org/10.1111/pace.14107>

Paige, C. F., Abbott, J. A., Elvinger, F. & Pyle, R. L. (2009): Prevalence of cardiomyopathy in apparently healthy cats. *J. Am. Vet. Med. Assoc.*, 234, 1398–1403.
<https://doi.org/10.2460/javma.234.11.1398>

Parto, P., Tadjalli, M. & Ghazi, S. R. (2010): Macroscopic and Microscopic Studies on Moderator Bands in the Heart of Ostrich (*Struthio camelus*). *Global Veterinaria*, 4, 374–379.

Perez, W. & Lima, M. (2007): Brief description of the cardiac anatomy in a tiger (*Panthera tigris*, Linnaeus, 1758): a case report. *Vet Med (Praha)*, 52, 83–86.
<https://doi.org/10.17221/2054-VET-MED>

Riesen, S. C., Doherr, M. G. & Lombard, C. W. (2007): Comparison of Doppler-derived aortic velocities obtained from various transducer sites in healthy dogs and cats. *Veterinary radiology & ultrasound*, 48, 570–573.

Sadek, M. M., Benhayon, D., Sureddi, R., Chik, W., Santangeli, P., Supple, G. E., Hutchinson, M. D., Bala, R., Carballeira, L., Zado, E. S., Patel, V. V., Callans, D. J., Marchlinski, F. E. & Garcia, F. C. (2015): Idiopathic ventricular arrhythmias originating from the moderator band:

Electrocardio-graphic characteristics and treatment by catheter ablation. *Journal of the Heart Rhythm Society and the Cardiac Electro-physiology Society*, 12, 67–75.

<https://doi.org/10.1016/j.hrthm.2014.08.029>

Thomas, W. P., Gaber, C. E., Jacobs, G. J., Kaplan, P. M., Lombard, C. W., Vet, M. & Moses, B. L. (1993): Recommendations for standards in transthoracic two-di-mensional echocardiography in the dog and cat. *Journal of veterinary internal medicine*, 7, 247-252.

Vazquez, N., Dos Santos, D., Pérez, W., Artigas, R. & Sorriba, V. (2019): Gross anatomy of the heart of Pampas's deer (*Ozotoceros bezo-articus*, Linnaeus 1758). *Journal of Morphological Sciences*, 36, 190–195.

<https://doi.org/10.1055/s-0039-1692159>

Wilkie, L. J., Smith, K. & Luis Fuentes, V. (2015): Cardiac pathology findings in 252 cats presented for necropsy; a comparison of cats with unexpected death versus other deaths. *J Vet Cardiol*, 17(Suppl 1), S329–S340.

<https://doi.org/10.1016/j.jvc.2015.09.006>

Wolf, O. A., Imgrund, M. & Wess, G. (2017): Echocardiographic assessment of feline false tendons and their relationship with focal thickening of the left ventricle. *Journal of Veterinary Cardiology*, 19, 14-23.

Wray, J. D., Gajanayake, J. & Smith, S. H. (2007): Congestive Heart Failure Associated with a Large Transverse Left Ventricular Moderator Band in Cats. *Journal Feline Medicine Surgery*, 9, 56-60.

<https://doi.org/10.1016/j.jfms.2006.03.006>

Corresponding Author:

Mohamed.om32@cu.edu.eg

Table (1): Internal morphometric measurements of right ventricular structures in centimeter (cm):

	N	Mean		Std. Deviation	Variance
		Value	Std. Error		
RAVD	5	1.2080	.04259	.09524	.009
RVD		1.2200	.07925	.17720	.031
PMCTL		.3340	.05528	.12361	.015

RAVD: Right atrioventricular valve diameter, **RVD:** Right ventricular diameter, **PMCTL:** Papillary magnus chordae tendinae length.

Table (2): External morphometric measurements of feline heart conformation in centimeter (cm):

	N	Mean		Std. Deviation	Variance
		Value	Std. Error		
A	5	5.1160	.24062	.53803	.289
B		3.2160	.19785	.44241	.196
C		1.0880	.11443	.25587	.065
D		2.4780	.11651	.26052	.068
E		3.5120	.18659	.41722	.174

a: distance between aortic arch & apex, **b:** heart base width, **c:** conus arteriosus diameter, **d:** distance from left auricle to apex, **e:** distance from right auricle to apex.

Table (3): Demographic and echocardiographic data of the admitted population:

Population characteristics	
Breed (n= 6)	
Persian cat	3
Domestic short hair	2
Domestic long hair	1
Gender	
Female	4
Male	2
Age (year)	6± 2.53
Weight (Kg)	2.7± 0.28
Heart rate and echocardiographic variables	
Heart rate (bpm)	164.16 ± 29.29
IVSd (mm)	3.73 ± 0.40
LVd (mm)	15.92 ± 1.03
LVPWd (mm)	4.17 ± 0.50
IVSs (mm)	7.07 ± 0.68
LVs (mm)	8.02 ± 2.16
LVPWs (mm)	6.83 ± 1.55
FS %	45.01 ± 14
EF %	82.98 ± 11.5
LA/Ao.	1.18 ± 0.15
MV E Vel. (cm/s)	68.82 ± 16.98
MV A Vel. (cm/s)	62.4 ± 9.83
MV E/A	1.22 ± 0.26
Ao. vel. (cm/s)	71.45 ± 10.54

bpm, beat per minute; IVSd, interventricular septal thickness at diastole; LVd, left ventricular chamber dimension at diastole; LVPWd, left ventricular posterior wall thickness at diastole; IVSs, interventricular septal thickness at systole; LVs, left ventricular chamber dimension at systole; LVPWs, left ventricular posterior wall thickness at systole; FS%, fractional shortening; EF, ejection fraction; MV E Vel., mitral inflow E wave velocity; MV A Vel., mitral inflow A wave velocity; MV E/A, mitral inflow E wave to A wave ratio; Ao, peak aortic velocity.

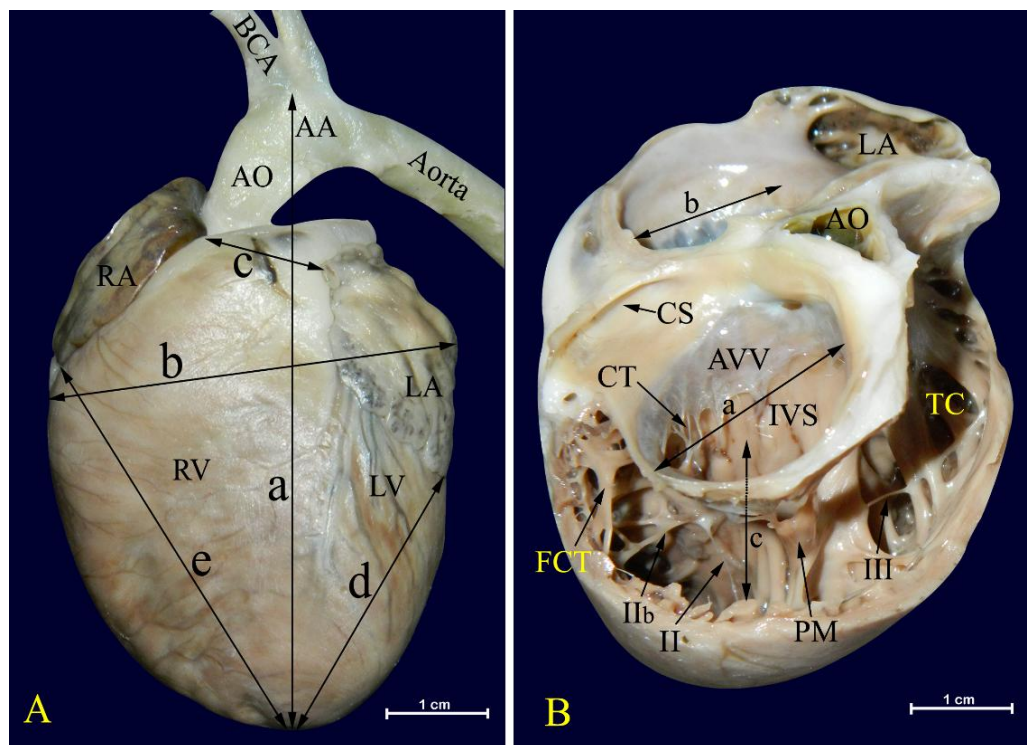


Fig.(1):A. Left lateral view of cat heart showing RA, right auricle. LA, left auricle. RV, right ventricle. LV, left ventricle. a, distance from aortic arch to apex. b, distance diameter of base. c, diameter of conus arteriosus. d & e, distances from ventral borders of auricles to apex. AO, ascending aorta. AA, aortic arch. BCA, brachiocephalic artery.

B. Dorsocranial view of opened right atrioventricular cavities showing septomarginal trabeculae of types II, IIb & III. a & b, right & left atrioventricular opening diameters. c, right ventricle diameter. LA, left auricle. AO, aorta. AVV, right atrioventricular valve cusp. CT, chordae tendineae. CS, coronary sinus. IVS, interventricular septum. TC, trabeculae carneae. PM, papillary magnus muscle. FCT, false chordae tendineae.

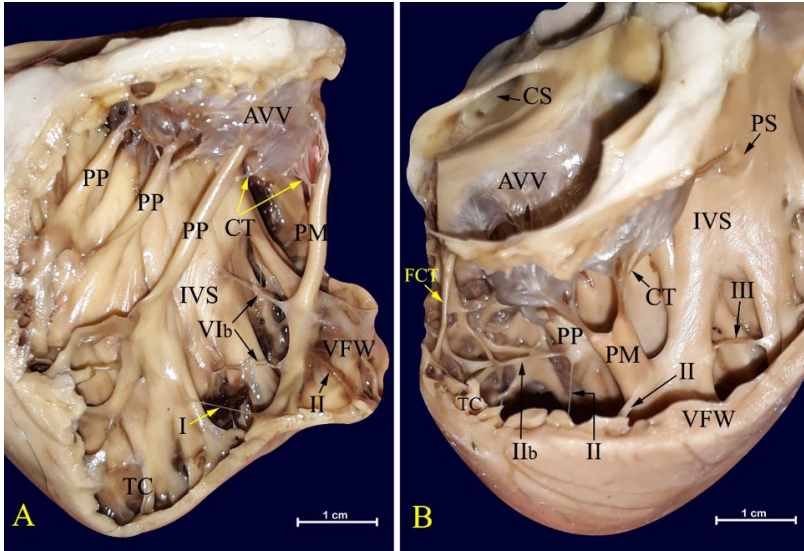


Fig.(2):A.Right lateral & B. left lateral views of cat right ventricle showing septomarginal trabeculae of types I, II, IIb, III & VIb. VFW, cutted ventricular free wall. AVV, atrioventricular valve cusp. CT, cordae tendineae. PP, papillary parvi muscles. PM, papillary magnus muscle. PS, papillary subarteriosus muscle. TC, trabeculae carneae. IVS, interventricular septum. FCT, false chordae tendineae. CS, coronary sinus.

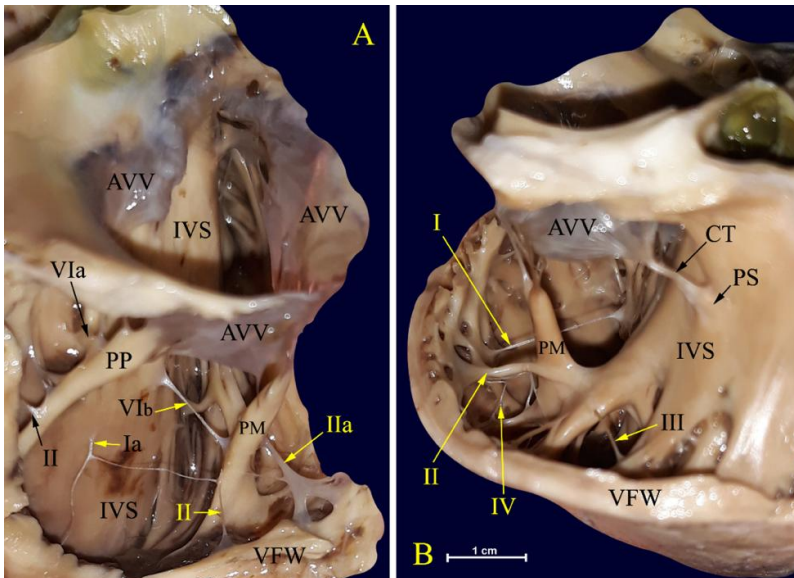


Fig.(3):A. Right lateral & B. left lateral views of cat right ventricle showing septomarginal trabeculae of types I, Ia, II, IIa, III, IV, VIa & VIb. VFW, cutted ventricular free wall. AVV, atrioventricular valve cusp. CT, cordae tendineae. PP, papillary parvi muscle. PM, papillary magnus muscle. PS, papillary subarteriosus muscle. IVS, interventricular septum.

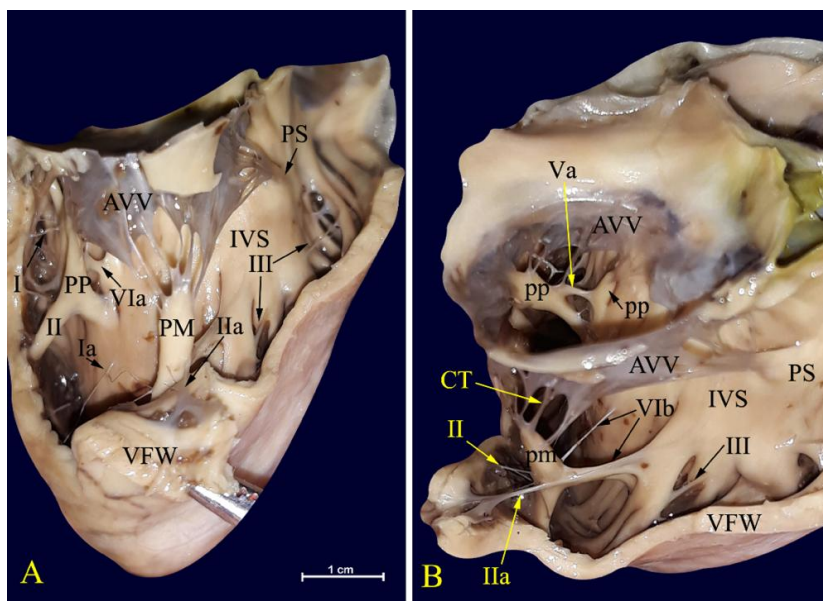


Fig.(4): A. Cranial & B. Right lateral views of cat right ventricle showing septomarginal trabeculae of types I, Ia, II, IIa, III, Va, VIa & VIb. VFW, cutted ventricular free wall. AVV, atrioventricular valve cusp. CT, cordae tendineae. PP, papillary parvi muscle. PM, papillary magnus muscle. PS, papillary subarteriosus muscle. IVS, interventricular septum.

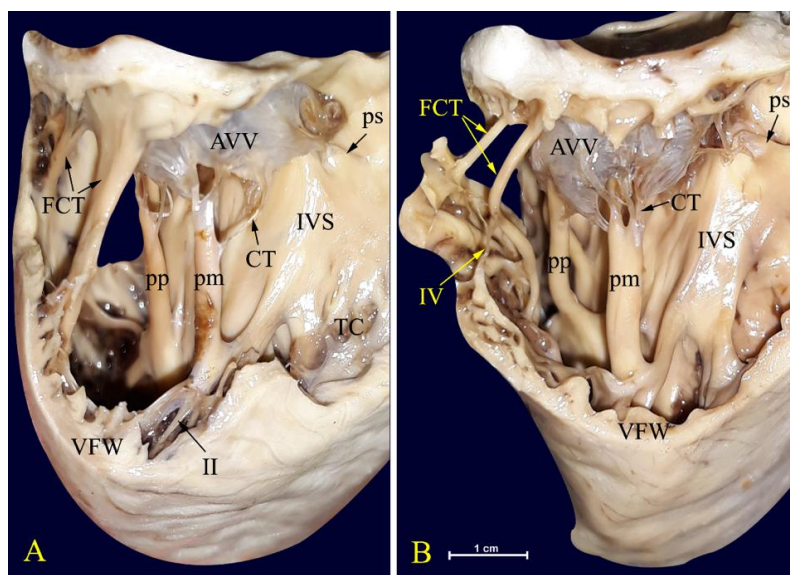


Fig. (5): A. & B. Left cranial views of cat right ventricle showing septomarginal trabeculae of types II & IV. VFW, cutted ventricular free wall. AVV, atrioventricular valve cusp. CT, cordae tendineae. PP, papillary parvi muscle. PM, papillary magnus muscle. PS, papillary subarteriosus muscle. IVS, interventricular septum. FCT, false chordae tendineae. TC, trabeculae carnaeae.

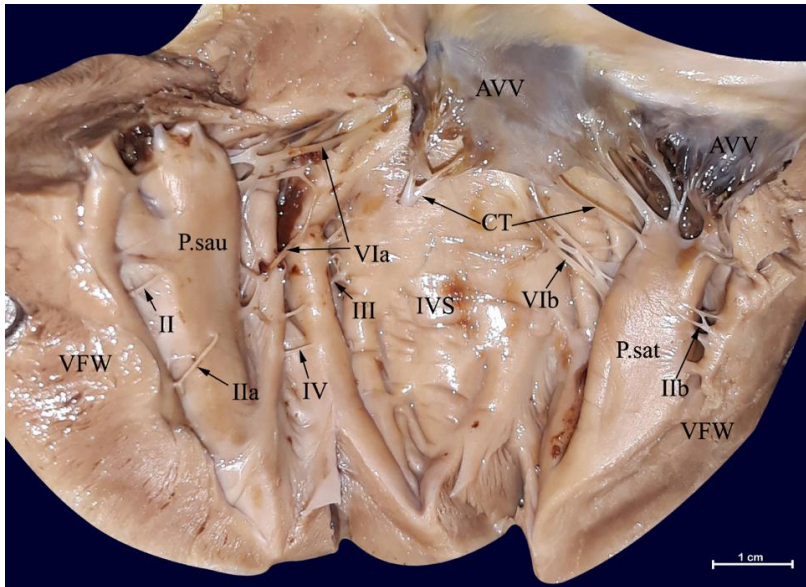


Fig. (6): Left ventricular cavity of cat showing septomarginal trabeculae of types II, IIa, IIb, III, IV, VIa & VIb. VFW, cutted ventricular free wall. AVV, atrioventricular valve cusp. CT, cordae tendineae. P.sau, papillary subauricularis muscle. P.sat, papillary subatrialis muscle. IVS, interventricular septum.

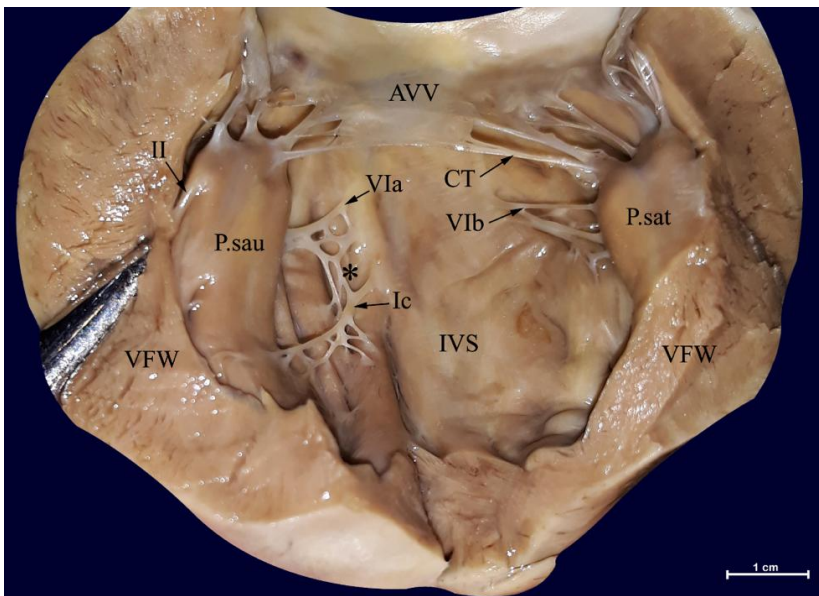


Fig. (7): Left ventricular cavity of cat showing septomarginal trabeculae of types Ic, II, VIa & VIb. VFW, cutted ventricular free wall. AVV, atrioventricular valve cusp. CT, cordae tendineae. P.sau, papillary subauricularis muscle. P.sat, papillary subatrialis muscle. IVS, interventricular septum. (*), connection between two trabecular types.

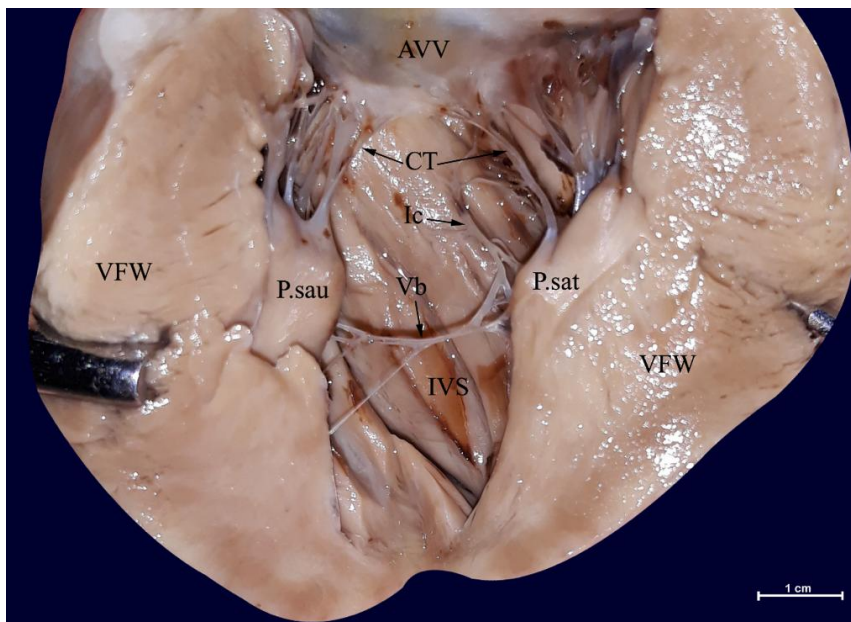


Fig. (8): Left ventricular cavity of cat showing septomarginal trabeculae of types Ic & Vb. VFW, cutted ventricular free wall. AVV, atrioventricular valve cusp. CT, cordae tendineae. P.sau, papillary subauricularis muscle. P.sat, papillary subatrialis muscle. IVS, interventricular septum.

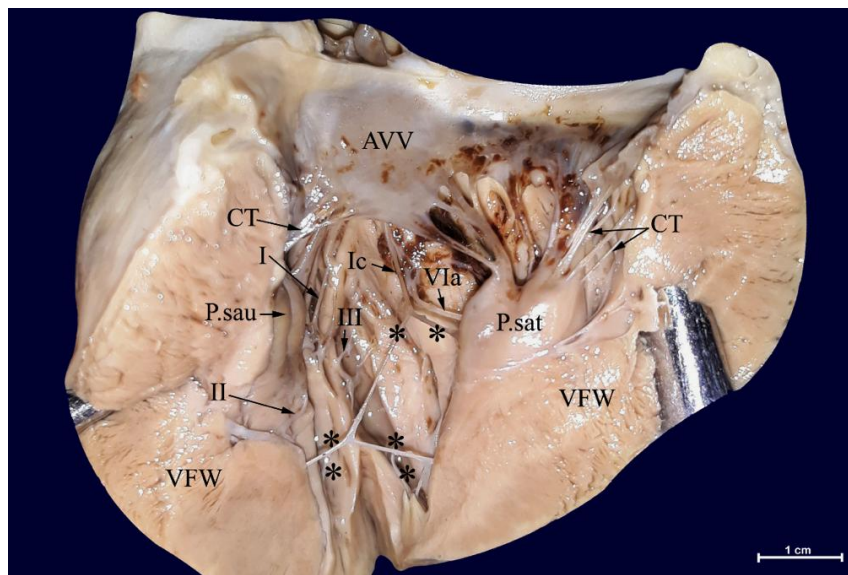


Fig. (9): Left ventricular cavity of cat showing septomarginal trabeculae of types I, Ic, II, III & VLa. VFW, cutted ventricular free wall. AVV, atrioventricular valve cusp. CT, cordae tendineae. P.sau, papillary subauricularis muscle. P.sat, papillary subatrialis muscle. IVS, interventricular septum. (*), branching pattern of type Ic.

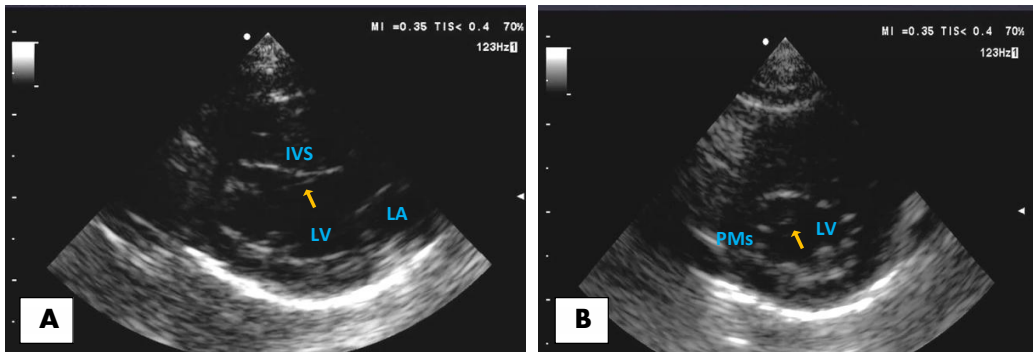


Fig. (10): (A) Echocardiographic image (foreshortened right parasternal long axis- five chamber view) of a seven-year-old healthy female Persian cat showing an echogenic fibromuscular band (yellow arrow) traversing the left ventricular chamber from the apex to the septum. (B) Right parasternal short axis- papillary muscle view showing the same band (yellow arrow) in cross section.

LA, left atrium; LV, left ventricular chamber; IVS, interventricular septum; PMs, papillary muscle.

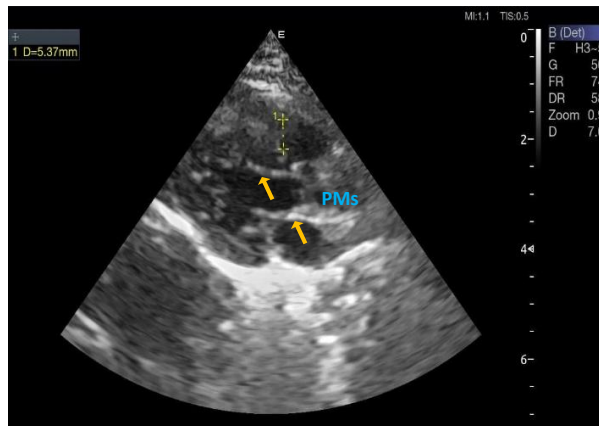


Fig. (11): Echocardiographic image (foreshortened right parasternal long axis- five chamber view) of a seven-year-old healthy female Persian cat showing the right parasternal short axis- papillary muscle view showing the same band (yellow arrow) in cross section. PMs, papillary muscle.

Source: Wikipedia, the free encyclopaedia

Animal species in this Issue

Domestic cat (*Felis catus* or *Felis silvestris catus*)



Kingdom: Animalia & Phylum: Chordata & Class: Mammalia & Order: Carnivora & Family: Felidae & Genus: *Felis* & Species: *F. catus*

The domestic cat is a small, usually furry, domesticated, and carnivorous mammal. It is often called a **housecat** when kept as an indoor pet. Cats are similar in anatomy to the other felids, with strong, flexible bodies, quick reflexes, sharp retractable claws, and teeth adapted to killing small prey. Cat senses fit a crepuscular and predatory ecological niche. Cats can hear sounds too faint or too high in frequency for human ears, such as those made by mice and other small animals. They can see in near darkness. Like most other mammals, cats have poorer color vision and a better sense of smell than humans.

The cat skull is unusual among mammals in having very large eye sockets and a powerful and specialized jaw. Within the jaw, cats have teeth adapted for killing prey and tearing meat. When it overpowers its prey, a cat delivers a lethal neck bite with its two long canine teeth, inserting them between two of the prey's vertebrae and severing its spinal cord, causing irreversible paralysis and death